Available online at www.sciencedirect.com
SCIENCE DIRECT®
Organic Geochemistry 36 (2005) 1117–1134
Organic Geochemistry
www.elsevier.com/locate/orggeochem

Microbial alteration of the acidic and neutral polar NSO compounds revealed by Fourier transform ion cyclotron resonance mass spectrometry

Sunghwan Kim [a], Lateefah A. Stanford [b], Ryan P. Rodgers [a], Alan G. Marshall [a,b,*], Clifford C. Walters [c], Kuangnan Qian [c], Lloyd M. Wenger [d], Paul Mankiewicz [d]

[a] *National High Magnetic Field Laboratory, Florida State University, Ion Cyclotron Resonance Program, 1800 East Paul Dirac Drive, Tallahassee, FL 32310-4005, USA*
[b] *Department of Chemistry and Biochemistry, Florida State University, Tallahassee, FL 32306, USA*
[c] *ExxonMobil Research and Engineering, 1545 Route 22 East, Annandale, NJ 08801-0998, USA*
[d] *ExxonMobil Upstream Research Company, PO Box 2189, Houston, TX 77252-2189, USA*

Received 14 December 2004; accepted 25 March 2005
(returned to author for revision 8 February 2005)
Available online 26 May 2005

Abstract

A suite of six genetically related oils that had experienced varying degrees of subsurface, anaerobic biodegradation was analyzed by ultrahigh-resolution Fourier transform ion cyclotron resonance mass spectrometry. By use of electrospray ionization of whole oil samples, all neutral nitrogen compounds and acid NSO compounds, from ~300 to 900 Da, are selectively characterized and assigned unambiguous molecular formulae. Several methods of data visualization reveal changes in the relative abundances of these compounds with increasing degradation.

Evidence for selective biodegradation is observed in all compound classes. NSO compounds associated with long alkyl side chains are removed, regardless of the NSO core, under conditions associated with moderate (saturated biomarkers unaffected) to severe biodegradation. Some compound series, such as O_1, O_3, and SO_{3-9}, are mineralized under conditions of mild biodegradation (*n*-alkanes, isoprenoids altered but still present). Changes in the Z-series (hydrogen deficiency) and alkyl distributions of the O_2 species result from simultaneous microbial degradation and generation. Acyclic fatty acids decrease, whereas $Z = -10$ O_2 species, which correspond to five-ring naphthenic (hopanoic) acids, increase in relative abundance during early stages of biodegradation. Monocyclic ($Z = -2$) O_2 are enriched initially, and then decrease during advanced stages of biodegradation. O_2 species corresponding to di-, tri-, and tetra-cyclic naphthenic acids ($Z = -4$, -6 and -8) are preferentially produced during these advanced stages. The ratio of acyclic to 2–4 ring cyclic O_2-species provides a new parameter to define the degree of biodegradation.

* Corresponding author. Tel.: +1 850 644 0529; fax: +1 850 644 1366.
E-mail address: marshall@magnet.fsu.edu (A.G. Marshall).

0146-6380/$ - see front matter © 2005 Elsevier Ltd. All rights reserved.
doi:10.1016/j.orggeochem.2005.03.010

1. Introduction

Petroleum biodegradation involves the degradation of hydrocarbons by surface and subsurface microorganisms. Most near-surface accumulations, such as the Orinoco and Western Canadian tar belts, are extensively degraded, having lost ~50–85% of their original hydrocarbon mass (Head et al., 2003). Biodegraded oils are commonly encountered in subsurface accumulations associated with reservoirs at low temperature (<80 °C) and with low water salinity (<100 ppt). There, either aerobic or anaerobic microbes may degrade petroleum following different biochemical pathways (Widdel and Rabus, 2001; Prince, 2002) at rates that depend strongly on the availability of inorganic and organic electron acceptors (Head et al., 2003; Larter et al., 2003; Holba et al., 2004). Complex interactions between the degrading petroleum, the reservoir environment and microbial populations result in the selective removal of certain compounds and the enrichment and/or generation of others. The overall effect is that semi-systematic changes in the chemical and physical properties of the residual crude oil and gases occur as biodegradation advances. Compared to unaltered equivalents, oils increase in specific gravity, become more viscous, and are richer in heteroatoms and metals with increasing severity of microbial alteration (Connan, 1984).

The relative susceptibility of saturated and aromatic hydrocarbons to microbial alteration is well documented (e.g., Volkman et al., 1983; Connan, 1984; Rowland et al., 1986; Hunt, 1995; Wenger et al., 2002; Peters et al., 2004). Briefly stated, the normal alkanes are catabolized preferentially, followed by branched alkanes, monocyclic saturated and monoaromatic hydrocarbons, multi-ring naphthenic and polynuclear aromatic hydrocarbons, and finally heteroatomic species. Differences in the susceptibility of hydrocarbons to microbial attack are seen within homologous series and even between isomeric forms (Peters et al., 1996; Townsend et al., 2004).

Less well documented are the effects of biodegradation on polar compounds. Limitations in reliable methods of detection and identification relegated prior studies to low molecular weight (<500 Da) species that are amenable to gas- or liquid-chromatographic analysis. Heteroatom-containing compounds generally are more resistant to microbial catabolism than are pure hydrocarbons. Some compounds, such as the vanadylporphyrins, appear to remain unaltered even in the most severely degraded oils (Sundararaman and Hwang, 1993). Other NSO compounds, such as carbazoles (Huang et al., 2003), quinolines (Benedik et al., 1998), dibenzothiophenes (Budzinski et al., 1998), and larger geomacromolecules (Jenisch-Anton et al., 2000; Pineda-Flores and Boll-Argüello, 2004) are biomineralized to varying degrees in laboratory and natural systems. Carboxylic acids are known to be generated during the biodegradation of crude oils under both aerobic and anaerobic conditions (Mackenzie et al., 1983; Behar and Albrecht, 1984; Jaffé and Gallardo, 1993; Thorn and Aiken, 1998; Meredith et al., 2000; Watson et al., 2002). These naphthenic acids can greatly impact oil producibility and economic value because they promote the formation of emulsions (Sjoblom et al., 2003) and the corrosion of metals (Slavcheva et al., 1999).

In this paper, we examine a suite of genetically related, biodegraded oils by electrospray ionization (ESI) coupled to high-field (9.4 T) Fourier transform ion cyclotron resonance mass spectrometry (FT-ICR MS). Positive-ion electrospray (i.e., protonation) ionizes basic nitrogen compounds (Hughey et al., 2001a; Qian et al., 2001a), whereas negative-ion electrospray (i.e., deprotonation) ionizes petroleum acids (Qian et al., 2001b; Hughey et al., 2002a) and weakly acidic, neutral nitrogen compounds (Hughey et al., 2002b). Neutral compounds, such as hydrocarbons, are not ionized. Hence, polar heteroatomic compounds are detected selectively despite the predominately non-polar hydrocarbon matrix of petroleum samples, eliminating the need for prechromatographic isolation. FT-ICR MS affords ultrahigh mass accuracy (<1 ppm) and resolving power ($m/\Delta m_{50\%}$ >350,000, in which $\Delta m_{50\%}$ denotes mass spectral peak full width at half-maximum height), allowing for the unambiguous assignment of molecular formulae of singly charged ions of 250–1000 Da (Marshall et al., 1998) for complex materials possessing more than 20 polar compounds per nominal mass.

This technique offers a very promising and powerful tool for detailed characterization of heteroatomic species in crude oils and crude oil distillates (Zhan and Fenn, 2000) and humic materials (Stenson, 2002; Kujawinski et al., 2002; Stenson et al., 2002; Kim et al., 2003b). We have previously resolved and identified more than 11,000 compositionally distinct polar components in a single mass spectrum for a crude oil (Hughey et al., 2002a). Negative-ion ESI FT–ICR mass spectra of three oils from different source facies (Hughey et al., 2002b) and two Smackover oils of different thermal maturity (Hughey et al., 2004) each yielded ~4000–8000 peaks that could be assigned to unique molecular formulae with high confidence. These identified compounds could be grouped into 18 heteroatomic classes, each containing a different combination of N, S and O atoms. Each compound class could be further defined by Z-series (hydrogen deficiency index) distributions representing molecules with similar core structures. Each Z-series, in turn, defines a homologous series of increasing number of methylene (CH_2) groups. Systematic variations at each level of specificity could be related to the influence of source and/or thermal maturity.

A major goal of our previous studies was to demonstrate the potential use of ultrahigh mass resolution and ultrahigh mass accuracy of FT-ICR MS for geochemical

applications and to familiarize geochemists with the technique. Here, we show continued development of the analytical technique, data processing and data visualization, and its application in characterizing the acidic and neutral polar NSO compounds in a suite of biodegraded oils. Many of the observed species and the changes in their distribution due to microbial alteration have not been previously documented.

2. Oil samples

Six oil samples were selected to represent petroleum subjected to different degrees of biodegradation under reservoir conditions (Table 1). These oils were analyzed by conventional methods and proved to be genetically related; that is, generated from similar, if not identical, source rocks (Mesozoic marine shales). Molecular distributions and basin model simulations indicate that these oils were generated and expelled under similar thermal conditions and have experienced comparable migration distances and reservoir charging conditions. The compositional differences within this oil suite are attributed mostly to biodegradation, although secondary influences cannot be discounted completely. All microbial processes are presumed to take place under anaerobic conditions because the geologic environment prohibits the influx of meteoric waters. Formation waters range from ~50 to 170 mg/g total dissolved solids.

Four of the six samples within the suite are described in Wenger et al. (2002) to illustrate the changes in the chemical and physical properties of crude oils subjected to subsurface biodegradation. These oils (samples 0–4) were collected during drill stem tests and are relatively free of contamination by drilling fluids. Two additional oils, samples 5 and 6, were added to the suite, extending the degree of biodegradation to severe and very severe conditions (Table 1). These samples were collected with a Reservoir Characterization Instrument and contain varying amounts of drilling fluid contaminants (primarily diesel fuel). Their genetic affinity to the less biodegraded samples is established from unaltered biomarker distributions (e.g., aromatized steroidal hydrocarbons) and geologic models of the local petroleum system.

The oil samples are identified by numbers that are roughly equivalent to the Biodegradation Indices described in Peters et al. (2004). The non-degraded oil is sample 0. Samples 1 and 2 exhibit characteristic initial preferential loss of *n*-alkanes, followed by sample 4 that exhibits a depletion of isoprenoid hydrocarbons with no discernable changes in saturated biomarker distributions (Fig. 1). Sterane distributions are altered in samples 5 and 6. Hopane and tricyclic terpene distributions in sample 5 are nearly identical to those seen in the less biodegraded oils. Hopane distributions are altered in sample 6, which also contains demethylated hopanes (Fig. 2).

Bulk physical and chemical properties and C_{15+} fractional compositions determined by HPLC separation are listed in Table 1. In general, the oils exhibit the expected trends associated with increasing microbial alteration: API gravity and saturated hydrocarbons decrease, whereas TAN (total acid number), sulfur, and nitrogen increase. Drilling fluids add ~C_{13}–C_{20} contaminants to samples 5 and 6; however, those additives will have little effect on the distribution of higher molecular weight polar compounds that are detected by the FTMS.

3. ESI–ICR–FTMS analysis

Sample preparation and ESI FT–ICR–MS analysis conditions were reported previously (Hughey et al., 2002a,b). In brief, sample solutions were prepared by dissolving oil samples in 50:50 toluene:methanol solvent at 1 mg/ml. A spike of 4 μL of NH_4OH was added to 1 ml of sample solution to ensure efficient ionization

Table 1
Geochemical properties of oil samples

Sample no. PM index	Degree of biodegradation	Sampling tool	°API	%S	N, ppm	$\frac{Ph}{n\text{-}C_{17}}$	Visc	TAN	C_{15+} group-type composition			
									%Sat	%Aro	%NSO	%Asph
0	None	DST	36.8	0.23	1220	.63	0.38	0.17	60.3	31.6	4.9	3.2
1	Slight	DST	31.8	0.24	1260	1.29	1.68	0.31	57.7	33.8	6.0	2.5
2	Moderate	DST	29.2	0.32	1200	3.89	1.50	0.48	59.0	34.0	6.0	1.0
4	Heavy	DST	21.4	0.42	1960	–	7.5	1.49	43.0	45.0	9.0	3.2
5	Severe	RCI	20.1	0.31	3470	–	n.d.	3.93	45.2	40.3	11.6	2.9
6	Very severe	RCI	11.8	0.68	2740	–	n.d.	5.50	37.2	45.4	14.4	3.0

PM index, Biodegradation Index from Peters et al. (2004), degree of biodegradation from Wenger et al. (2002); DST, drill stem test; RCI, reservoir characterization instrument (Baker–Hughes); Visc., live oil reservoir viscosity, cp; °API = (141.5/s.g.) – 131.5 where s.g., specific gravity: density relative to pure water. TAN, total acid number, mg KOH/g oil, C_{15+} group-type composition separation method described in (Isaksen, 1996). %Sat, wt% saturated hydrocarbons; %Aro, wt% aromatic hydrocarbons; %NSO, wt% polar compounds. %Asph., wt% asphaltenes. Sample #6: the reported data is for a mixture of diesel and biodegraded oil.

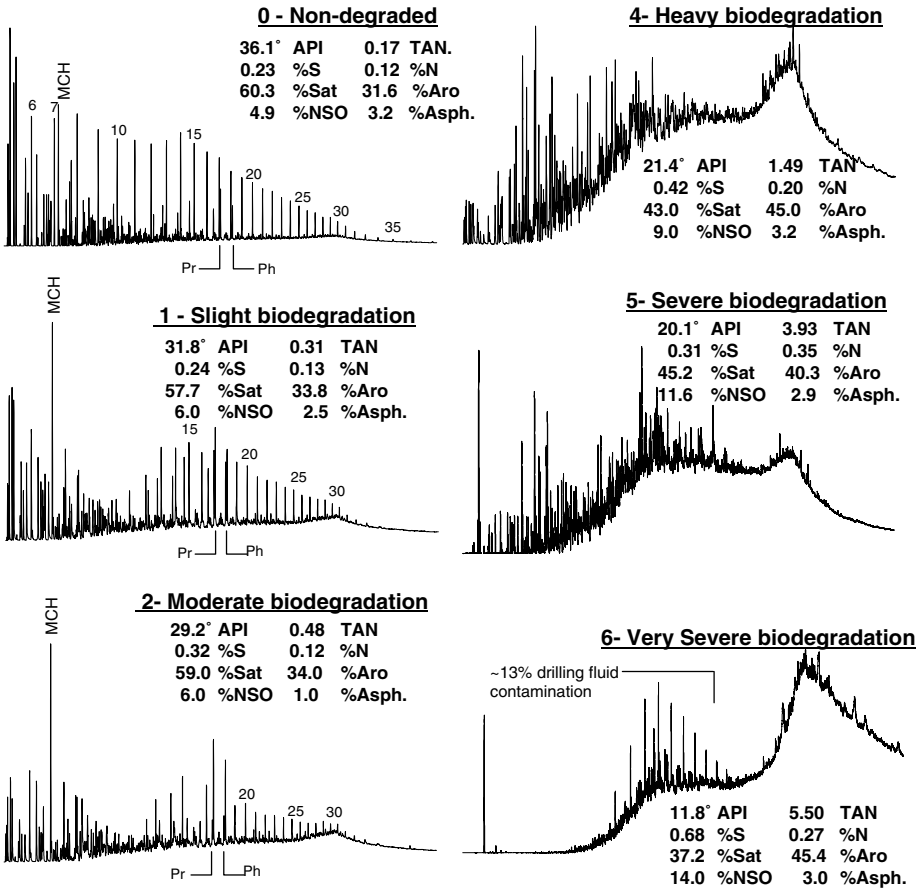

Fig. 1. Whole oil gas chromatograms of a suite of genetically related oils that differ in degree of biodegradation. Sample numbers correspond to the Biodegradation Index from Peters et al. (2004). See Table 1 for notation. Samples 0–4 are from drill stem tests; samples 5–6 were recovered by a Reservoir Characterization Instrument (Baker-Hughes) and are contaminated by drilling mud additives. See (Isaksen, 1996) for instrumental conditions.

(deprotonation) for negative-ion electrospray analysis. The sample was introduced into a micro-electrospray source (Emmett et al., 1998) at a flow rate of 400 nl/min, under typical conditions for formation of negative ions (50 μm i.d. fused silica needle, 2 kV needle voltage, 300 V tube lens, 4 A heated capillary current).

A homebuilt FT–ICR mass spectrometer equipped with a 222 mm horizontal room temperature bore 9.4 T magnet (Senko et al., 1996b) was used in these experiments. Ions generated in the ESI source region are first accumulated in an external linear octopole ion trap for 20–60 s and transferred through rf-only multipoles to a 10 cm diameter, 30 cm long open cylindrical Penning ion trap (Senko et al., 1997). Multipoles (Hendrickson et al., 2000) were typically operated at 1.7 MHz at a peak-to-peak rf amplitude of 170 V. After ions were excited in the trap by broadband frequency-sweep (chirp) dipolar excitation (70–641 kHz at a sweep rate of 150 Hz/μs and amplitude, 190 V_{p-p}), direct mode image current detection was performed to yield 4 Mword time-domain data. Time domain data sets were co-added (200 acquisitions) and then Hanning apodized, followed by a single zero-fill before fast Fourier transformation and magnitude calculation. Frequency was converted to mass-to-charge ratio by the quadrupolar electric trapping potential approximation (Ledford et al., 1984; Shi et al., 2000). Data acquisition and processing was conducted with a MIDAS system (Senko et al., 1996a; Blakney et al., 2001).

Mass spectra were externally calibrated with respect to a G241A Agilent (Palo Alto, CA) electrospray "tuning mix". Mass values obtained from the calibrated spectra were then converted to Kendrick mass and sorted according to Kendrick mass defect values (Kendrick, 1963). Peak assignments were performed by Kendrick mass defect analysis as previously reported (Hughey et al., 2001b). Briefly, an elemental formula is assigned to peaks of lowest *m/z* value at each Kendrick mass

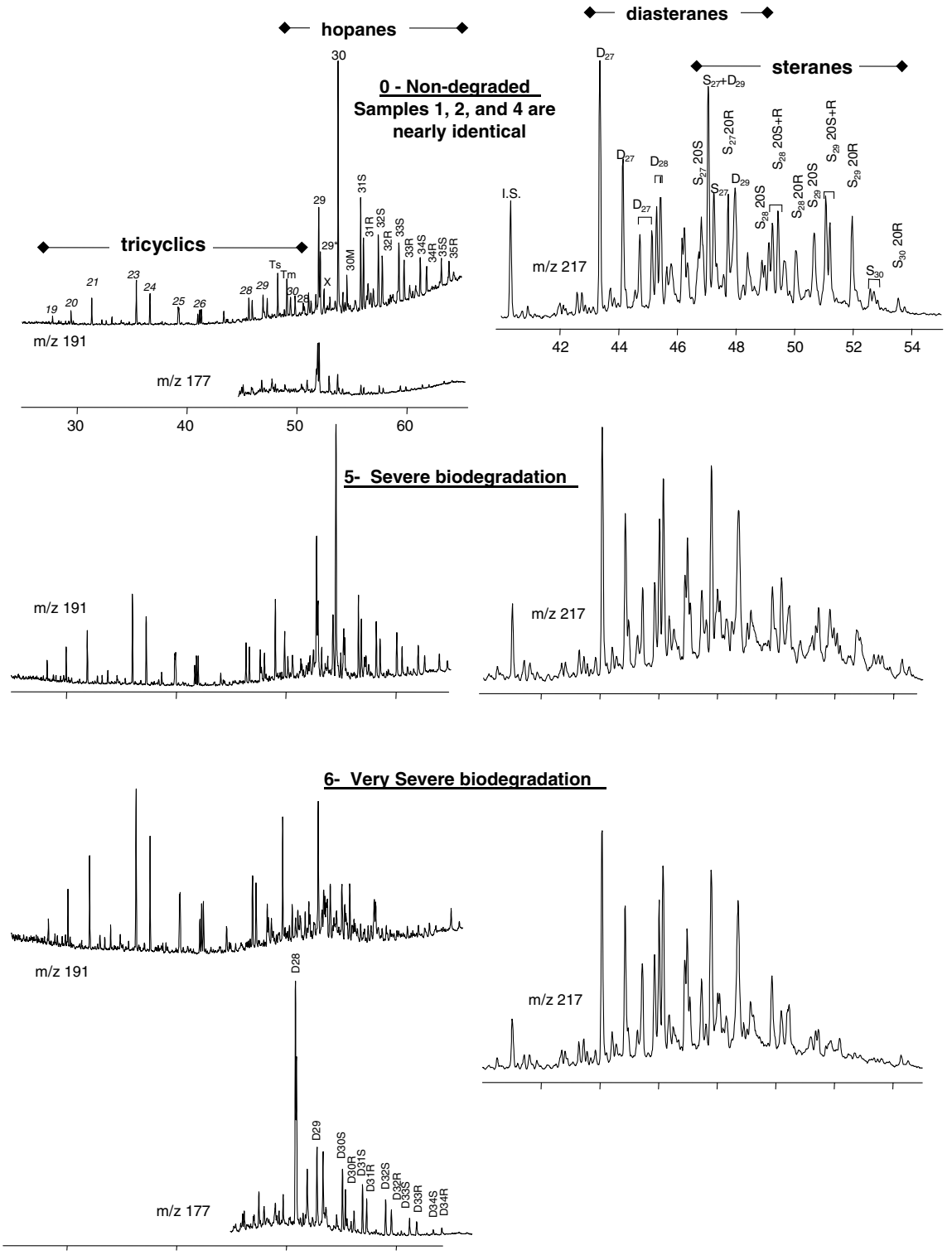

Fig. 2. Reconstructed ion chromatograms showing tricyclic and pentacyclic terpanes (*m/z* 191), and steranes and diasteranes (*m/z* 217) for selected samples. The presence of demethylated hopanes in the most biodegraded sample (6) is noted in the diagnostic *m/z* 177 ion trace (abundance plotted relative to *m/z* 191 peak magnitude). See (Isaksen, 1996) for instrumental conditions.

defect number. Elemental compositions are restricted to C, H, O, N, S, ^{13}C and ^{34}S atoms. Higher-mass peaks are assigned by adding multiples of CH_2 to the designated elemental formula.

The calibrated negative-ion FT-ICR mass spectra of four representative samples are presented in Fig. 3. In each spectrum, more than 3000 peaks with a signal to noise ratio of 5 are detected in the range, $300 < m/z < 800$ at an average mass resolving power of more than 400,000. The broadband mass spectra clearly show that the molecular weight distribution of polar compounds is greatly influenced by biodegradation. The weight-average molecular weight is relatively constant at 539 ± 4 Da for samples 0–2 and decreases with biodegradation to 470, 462 and 460 Da for samples 4 through 6, respectively.

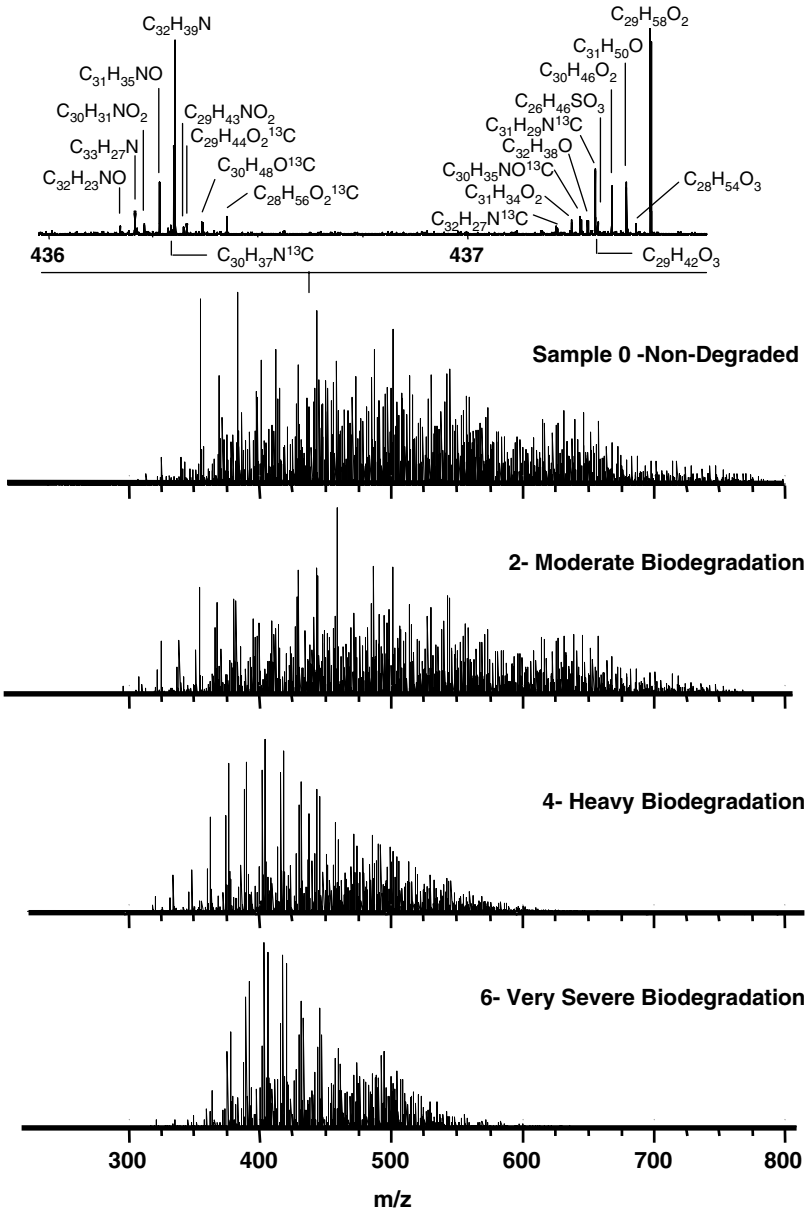

Fig. 3. Broadband negative-ion electrospray ionization 9.4 T FT-ICR mass spectra of crude oils at distinct stages of biodegradation: non-degraded (0), moderately degraded (2), heavily (4) and very severely degraded (6) genetically related oils. To show the complexity of the spectra, one mass scale-expanded segment is displayed at the top of the diagram.

4. Results and discussion

Biodegradation alters the distribution of saturated and aromatic hydrocarbons by selective removal, whereas the distribution of acidic and neutral nitrogen polar compounds is altered by selective removal, preservation and generation. These alterations are observed at all levels of investigation; that is, between compound classes, Z-series within classes and alkylated homologues within a Z-series. Furthermore, microbially induced alteration of the polar compounds appears to produce systematic changes, suggesting that selected NSO-class or compound ratios can be used as indices to evaluate the extent of biodegradation.

4.1. Compound class distribution

The distribution of summed compound classes in the non-degraded oil (sample 0) is similar to that reported previously for oil derived from a marine shale source (Hughey et al., 2002b) (Fig. 4). N-compounds are the predominant species, followed by O−, O_2 and NO-compounds. Other heteroatomic species, including those containing sulfur, are present in comparatively minor amounts.

Biodegradation alters the compound class distributions to different degrees. O, O_3, O_4, NO, N_2O, SO_2, SO_3 and NS species tend to decrease whereas O_2, SO, S_2O species increase with increasing biodegradation. The increase in O_2-species is most predominant in the heavily to severely biodegraded oils (samples 4–6); and, as discussed below, is attributed to the creation of naphthenic acids via partial oxidation of hydrocarbons. The addition of O_2-species results in a corresponding decrease in the relative abundance of other species. Hence, some compound classes (N and N_2) that appear to decrease may actually remain fairly constant in absolute abundance and are simply diluted by addition of O_2 and other species.

Because different compounds have different ionization efficiencies, detailed quantification is not possible without extensive additional quantitation with known (and/or isotopically labeled) compounds, many of which are not commercially available. Therefore, in this paper, discussion of class distribution is focused on comparing similar kinds of molecules in samples at different states of degradation. Fig. 4 should be interpreted accordingly.

4.2. O-containing Z-series distributions

The greatest changes imposed by biodegradation occur for species containing oxygen. The overall effects are similar to those seen for aromatic hydrocarbons; that is, increased bioresistance with increasing ring-number and aromaticity. The actual distributions change in a complex fashion as Z-series acids (O_2) are preserved, consumed and generated.

4.2.1. Changes in O_1 species

$C_nH_{2n+z}O$ species are relatively abundant in the non-degraded oil (sample 0) beginning and maximizing at $Z = -6$, likely corresponding to phenols or aromatic alcohols rather than aldehydes. Abundance gradually decreases with increasing Z-number, with mass peaks detectable to $Z \approx -38$, corresponding to a 6.5-ring aromatic system (Fig. 5).

With the onset of biodegradation, the relative abundance of $C_nH_{2n+z}O$ species diminishes in roughly inverse proportion to the number of double bond equivalents (DBE). O-compounds with monoaromatic

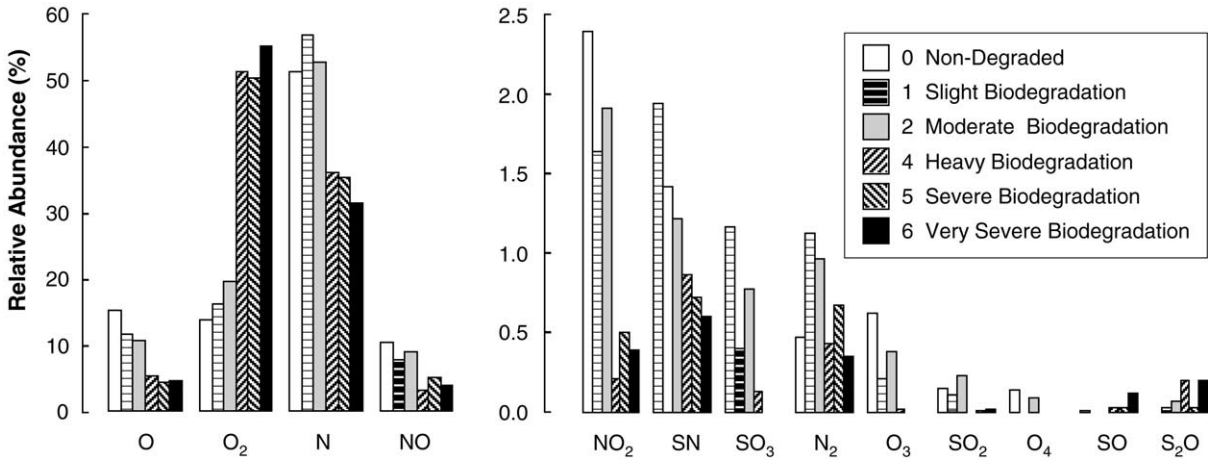

Fig. 4. Relative abundances of compound classes identified in a suite of genetically related oils microbially degraded to different degrees. Sample number corresponds to the Biodegradation Index (Peters et al., 2004).

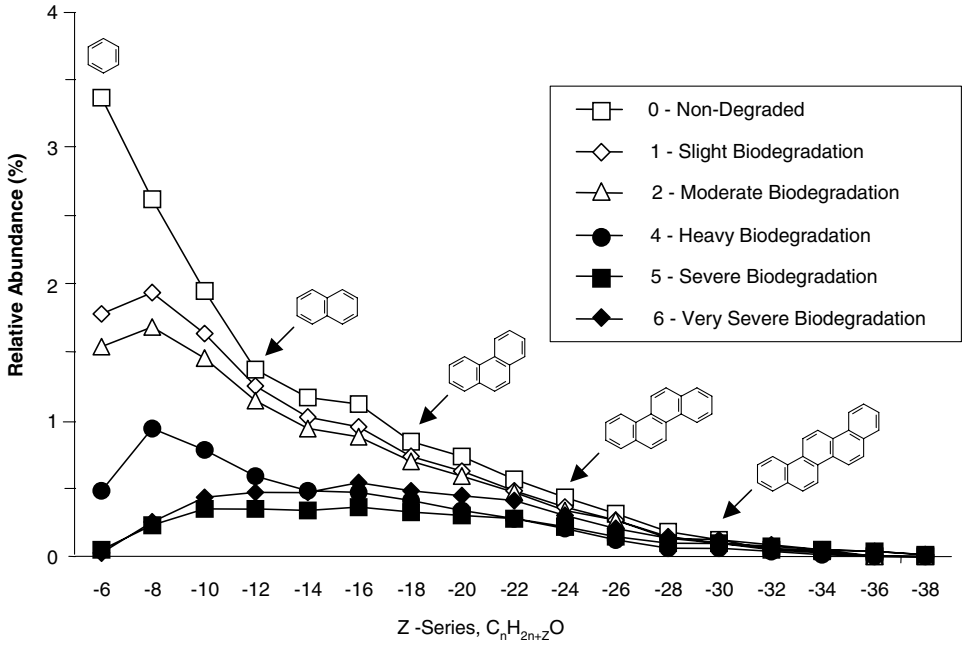

Fig. 5. Z-series abundance distribution of $C_nH_{2n+z}O$ compounds for each of several extents of biodegradation. Fully aromatized hydrocarbons are shown as representative cores, although naphthenic-aromatic cores with identical double bond equivalents may also be present. ^{12}C and ^{13}C isomers are combined.

cores ($Z = -6$) decrease by about half in oils that are only slightly and moderately biodegraded (samples 1 and 2) and are nearly absent in the severely degraded oils (samples 5 and 6). The decrease in phenolic and/or benzylic O-species is attributed to biodegradation rather than to water washing because preferential preservation is not observed with increasing alkylation in the $Z = -6$ series. O-species with higher DBE values ($-6 > Z > -22$) persist even in the severely biodegraded oils, although at reduced concentrations. O-species with four or more aromatic cores (or equivalent larger aromatic-naphthenic ring structures, $Z \leqslant -24$) are largely unaffected by biodegradation, although their relative abundances are reduced by acid dilution.

4.2.2. Changes in O_2 species

$C_nH_{2n+z}O_2$ species with one double bond equivalent ($Z = 0$) dominate the Z-series distribution for the non-degraded oil (sample 0, Fig. 6). These molecules can be assigned only as acyclic fatty acids. The next most abundant series is $Z = -10$, corresponding to core hydrocarbons with five saturated rings or to tetralins (tetrahydronaphthalenes), followed by $Z = -8$, corresponding to acids with core hydrocarbons with four saturated rings or benzene.

Some alteration of the O_2 species distributions is seen even for the slightly biodegraded oil (sample 1). The overall total abundance of O_2 species increases slightly, but the relative distribution of the $Z = 0$ series (fatty acids) decreases whereas the $Z = -2$ to -12 relative abundances increase. Curiously, relative abundances of series with a higher number of double bonds ($Z > -12$) also decrease slightly. These trends continue in the moderately degraded oil (sample 2) until the $Z = -2$ (monocyclic) and $Z = -10$ (pentacyclic) are more abundant than the fatty acids.

The nature of the O_2-species distribution changes more dramatically on further biodegradation (samples 4–6). Acyclic fatty acids steadily decrease to trace levels in the mostly severely degraded oil. One- to three-ring cyclic naphthenic acids ($Z = -2$ to -6) become dominant and originally prominent five-ring species ($Z = -10$) decrease in significance. The distribution of these cyclic naphthenic acids shifts with increasing biodegradation from predominance of 1-ring in the heavily degraded oil (sample 4), to 2-rings in the severely degraded oil (sample 5), and finally to 3-ring in the most degraded oil (sample 6).

Although ESI–FT ICR MS provides highly detailed information on the various heteroatom-containing compounds, an obvious limitation of the technique is that isomers cannot be distinguished by mass alone. However, the assignment of the $Z = 0$ to -10 O_2 series to acids with hydrocarbon cores of 1–5 saturated rings is reasonable. The designation of the $Z = -10$ series primarily to hopanoic acids is supported by prior

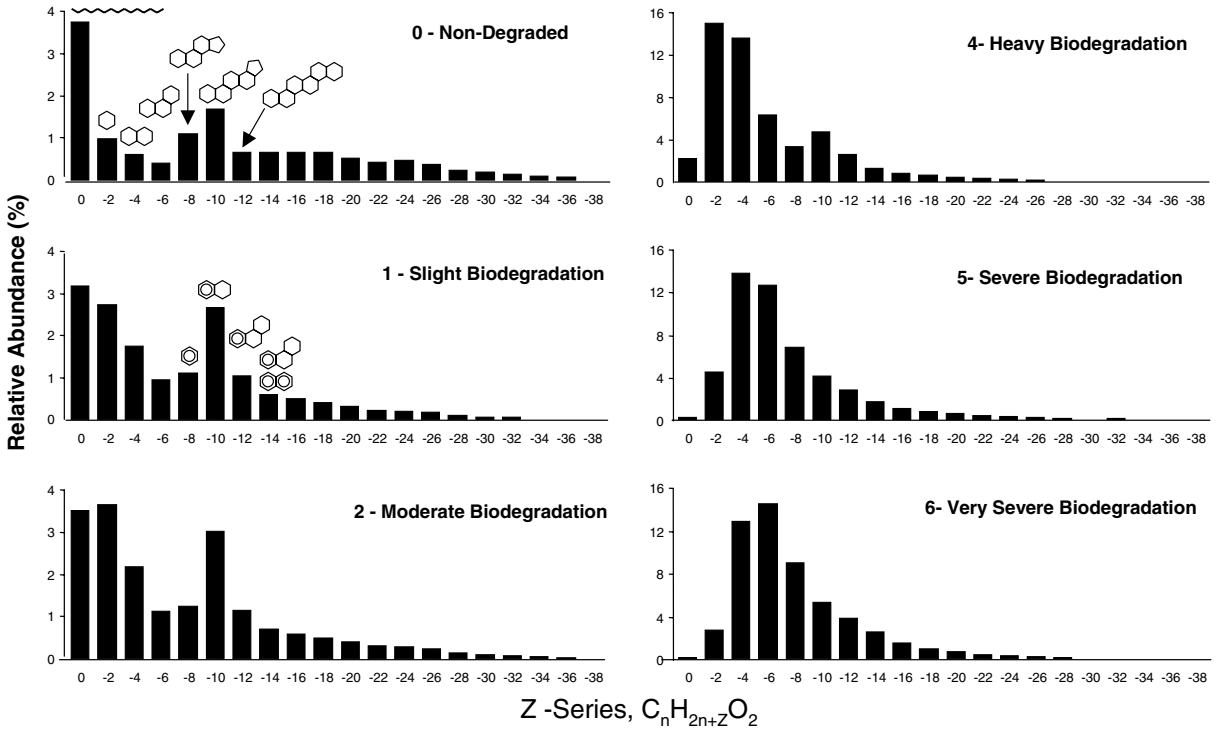

Fig. 6. Z-series abundance distribution of $C_nH_{2n+z}O_2$ compounds due to extent of biodegradation. Structures of representative hydrocarbon cores are shown for $Z = 0$ to -10. ^{12}C and ^{13}C isomers are combined.

correlations of the abundance of hopanoic acids with increasing microbial alteration (Nascimento et al., 1999; Meredith et al., 2000; Watson et al., 2002). The alkyl distributions seen in the high-resolution mass spectra resemble the pattern observed by Meredith et al. (2000) (Fig. 7). C_{32} and C_{31} hopanoic acids are enriched upon mild to moderate biodegradation. The C_{30} and lower hopanoic acids become more dominant as biodegradation becomes more severe. Hopane distributions remain constant with no significant indication of demethylation until very severe biodegradation (sample 6) in which the hopanes have been largely converted to demethylated forms (Fig. 2). The alkyl distribution of the $Z = -10$ O_2 series in Fig. 6 appears to reflect this carbon number shift with the C_{29} species being most dominant.

We speculate that the apparent changes in hopanoic acid distributions reflect changes in microbial pathways as biodegradation proceeds. The enrichment of C_{31} and C_{32} hopanoic acids under mild to moderate biodegradation, followed by C_{30} hopanoic acid predominance under more severe degradation (concurrent with no obvious depletion of hopanes) suggests that the hopanoic acids are being generated by the degrading bacteria and that the microbial population is changing. In contrast, the severely biodegraded oil appears to be oxidizing the demethylated hopanes into their acid equivalents or preferentially consuming the C_{30+} hopanoic acids to enrich the lower species. This shift in hopanoic acid distribution suggests that another microbial population, possibly composed of *archaea* or non-hopanoid-producing bacteria, becomes dominant under such conditions.

4.2.3. Changes in O_3 and O_4 species

Similar shifts in Z-distribution (not shown) are observed for the O_3 and O_4 species as for the O_2 species. The O_3 and O_4 species are most abundant in the non-degraded oil: O_3 species are relatively minor; the $Z = 0$ acyclic species are the most prominent; and O_4 species are trace components. O_3 species tend to diminish with increasing biodegradation and drop below the limit of detection in the severely and very severely biodegraded oils. O_4 species rapidly fall below the limit of detection even in the slightly biodegraded oil. These observations contrast with those made by Tomczyk et al., (2001) for a severely biodegraded San Joaquin Valley oil, for which O_4 species were nearly equal in abundance to O_2 species, and O_5 and O_6 species were approximately half the abundance of O_2 species. Tomczyk et al. (2001) attributed the high oxygen content to aerobic conditions.

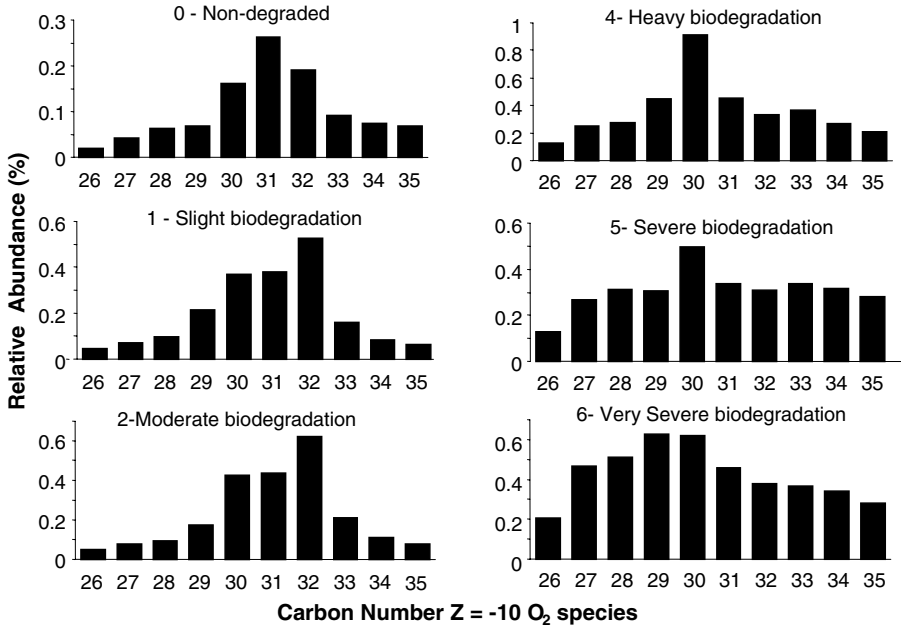

Fig. 7. Alkyl distribution by carbon number (C_{26}–C_{35}) for the $Z = -10$ series for O_2 species, for each of several degrees of biodegradation. Although the distribution of hopanoic acids changes with increasing biodegradation, the distribution of hopanes remains essentially constant for samples 0–5. Only for the most severely biodegraded oil (sample 6) are hopanes depleted and demethylated hopanes formed (see Fig. 2).

4.2.4. Modified van Krevelen diagrams for O-species

A modified van Krevelen plot offers a convenient graphical display to study and compare complex mass spectra (Kim et al., 2003a; Wu et al., 2003). These plots are constructed as contour maps, with contours color coded according to relative abundance, for the H/C and O/C (or the N/C or S/C) ratio of each assigned elemental formula (Figs. 8 and 10). Such plots make it easy to recognize changes in relative abundance of various heteroatomic classes, Z-distributions, and alkylation distributions, all in a single display. For example, the H/C ratio increases and the O/C ratio decreases with increasing alkylation for each individual Z-series, as shown by the diagonal straight lines overlaid on Fig. 8.

The modified van Krevelen plots readily illustrate the influence of biodegradation on distribution of O-species. O species diminish to low levels in the highly degraded oils (samples 4–6). O_3^+ is present at a lower level than other species and decreases even more as biodegradation proceeds. The disposition of the O_2-species varies according to Z-series and degree of alkylation. Acyclic ($Z = 0$) acids are removed under the mildest degree of alteration and are eliminated almost completely in the most severely degraded samples. O_2 species with DBE values of 2, 3 and 4 ($Z = -2$, -4 and -6) increase with increasing biodegradation and probably represent partial oxidation of mono-, di-, and tri-cyclic saturated hydrocarbons. O_2 species with DBE values of five follow the same trend, but may be less diagnostic because they represent a composite of carboxylated tetracyclic naphthenes and tetralins. O_2 species with DBE values of 6 ($Z = -10$) increase in relative abundance and then decrease in significance, indicative of the selective addition of hopanoic acids from bacterial biomass.

Also notable is an apparent decrease in O_2 species for species of relatively low H/C ratios ranging from 1 to 1.5 ($Z < -12$) corresponding to highly cyclic or aromatic acid molecules. That apparent decrease in relative abundance is due in part to the generation of $Z > -12$ naphthenic acids that dilute the remaining O_2 species. Whether this dilution can account for all of the variance or highly condensed O_2 species are being selectively consumed is as yet undetermined.

4.2.5. A new Biodegradation Index based on O_2-species distribution

The consistent decrease in acyclic fatty acids and increase in cyclic O_2 species suggest that these compounds could be used as a measure of the degree of biodegradation. The A/C ratio (acyclic to cyclic naphthenic acids) is calculated from the sum of mass spectral peak magnitudes of the acyclic (DBE = 1, $Z = 0$) O_2 species divided by the sum of magnitudes of the mono, di- and tri-cyclic acids (DBE = 2, 3 and 4; $Z = -2$, -4 and -6, respectively). The A/C ratio appears to correlate well with degree of biodegradation of crude oil (Fig. 9), which is a

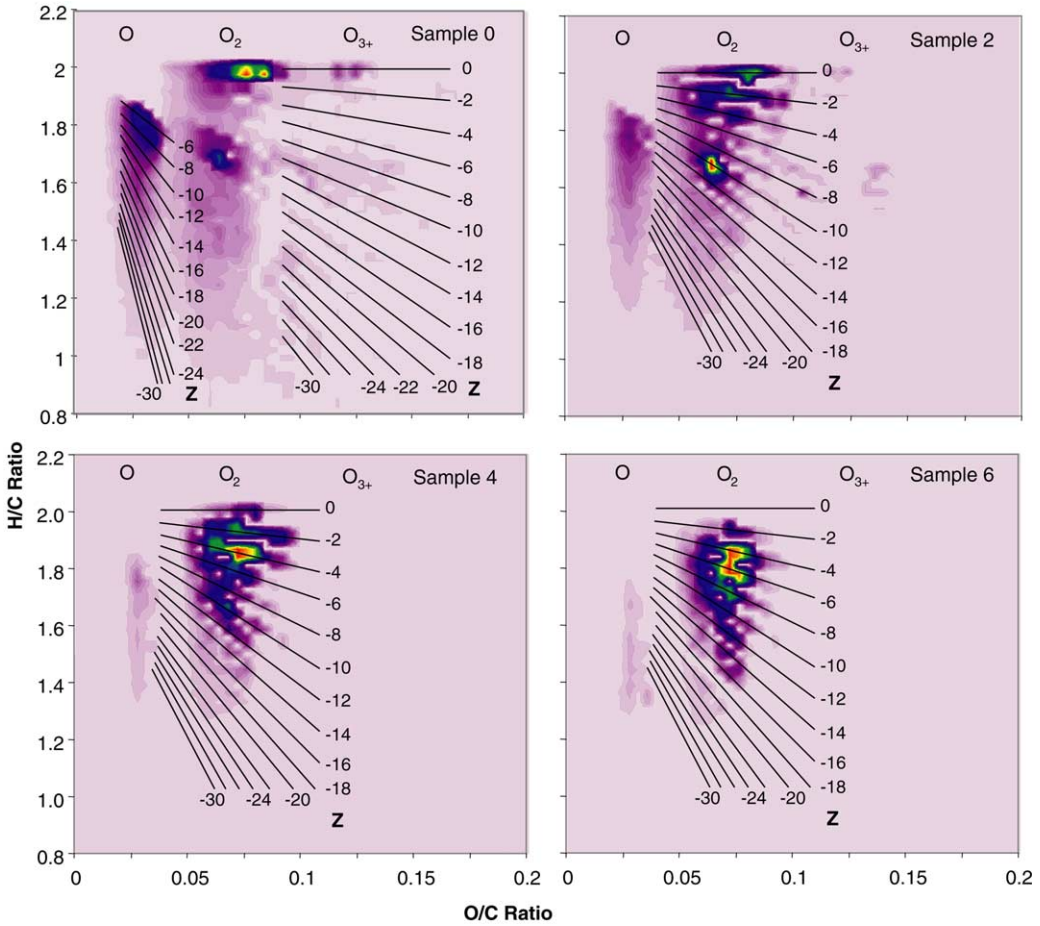

Fig. 8. 3D van Krevelen diagram of oxygen-containing compounds identified in non-degraded (sample 0), slight-moderately degraded (sample 2), severely degraded (sample 4) and very severely degraded (sample 6) genetically related oils. Normalized ion abundance is color coded by peak height (light purple = minimum, red = maximum). Z-series trend lines for $C_nH_{2n+z}O$ are shown for sample 0. Z-series trend lines for $C_nH_{2n+z}O_2$ are shown for samples 2, 4, and 6. $Z = +2$ for acyclic fatty acids. $Z = -8$ for hopanoic acids. Alkylation within individual Z-series increases from right to left.

qualitative description notwithstanding its numerical labeling. As such, the A/C ratio could potentially provide a more reliable, quantitative measure of the degree of biodegradation and offer additional insight into reservoir fill histories where biodegraded oils are recharged with non-degraded petroleum fluids. Studies of additional biodegradation suites will be needed to verify the broader applicability of the A/C ratio.

4.3. Nitrogen-containing compounds

As discussed earlier, nitrogen-containing compounds, mainly N_1 species, are dominant in the non-degraded oil and become progressively less abundant relative to O-species as biodegradation proceeds (Fig. 4). This decrease in relative abundance of N_1-species may be attributed to the addition of O_2 and other species, decreased sensitivity for N_1-species due to reduced ionization efficiency in the presence of other species, or microbial consumption of nitrogen compounds. If the relative decrease of N_1-species were due to dilution or impaired ionization, then the internal Z-distributions for those compounds should remain fairly constant on biodegradation. However, modified van Krevelen plots show clear changes in the Z-series distribution for the N_1-species with increasing biodegradation (Fig. 10). Carbazoles and benzocarbazoles ($Z = -21$) dominate the non-degraded and mildly biodegraded oils, but diminish relative to N_1-species with higher DBE values on more severe biodegradation.

Fig. 11 shows contours of relative abundance of N_1 species for Z-distribution versus carbon number distribution, allowing for correlation between those two

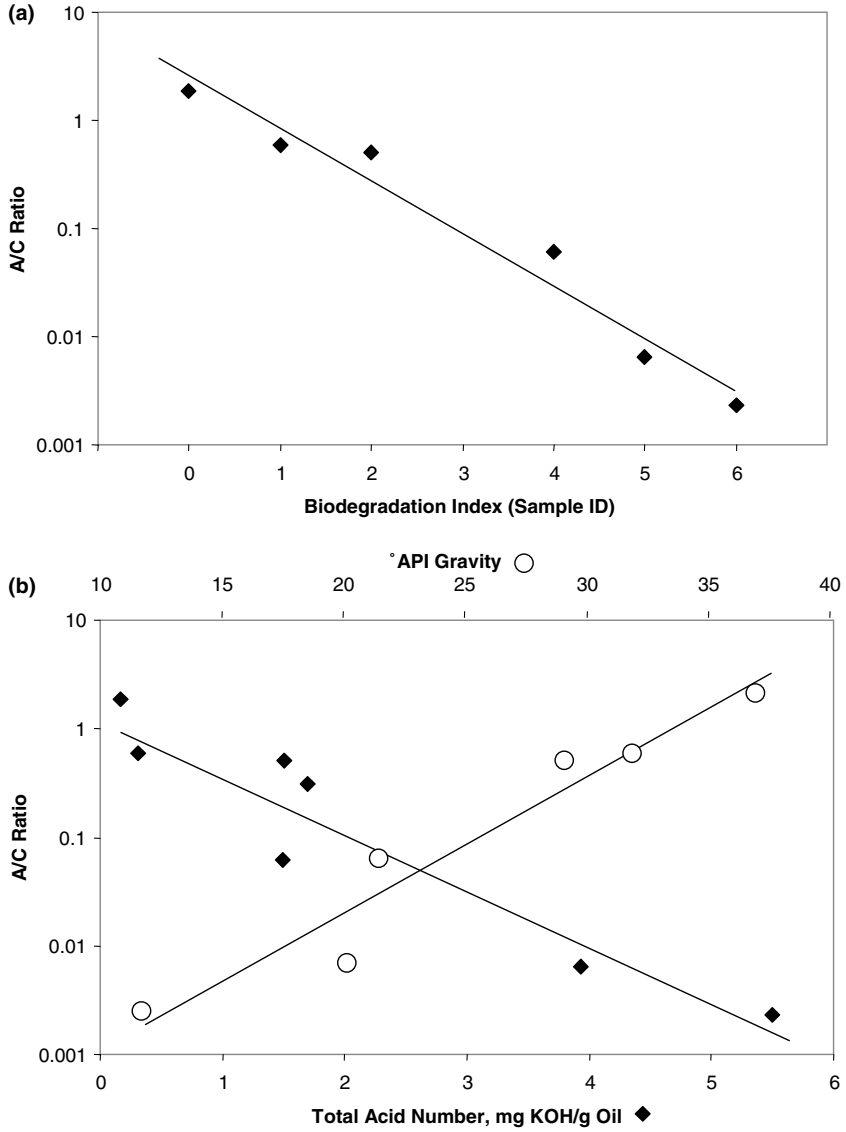

Fig. 9. (a) Correlation between the A/C ratio (acyclic/Σ(2–4 ring cyclic) O_2 species) and the Biomarker Biodegradation Index (Peters et al., 2004). (b) A/C ratio as a function of API gravity or total acid number.

molecular properties. Although little change in either property occurs following mild biodegradation, N_1 compound distributions alter substantially in oils subjected to greater microbial activity. Most obvious is the reduced degree of alkylation in all Z-series, suggesting that degrading enzymes are attacking long alkyl sidechains as if they were alkanes. Selective destruction of the pyrrolic cores is apparent in the most severely degraded oil, as the maximum abundance shifts from $Z = -21$ (benzocarbazole) to species with higher DBEs. Species in the $Z = -23$ and -25 series include compounds with either additional naphthenic rings, pendant phenyls, or more condensed pyrrolic cores. The latter group is likely to be the most resistive to biodegradation.

Microbial degradation of N_1 compounds can yield a host of possible compounds, and the susceptibility to degradation depends on the position and/or placement of the nitrogen atom in five- or six-member rings. The biodegradation of carbazoles by aerobic bacteria is known to involve the breaking of the aromatic or cyclic ring containing the nitrogen, removing the nitrogen and replacing it with hydroxyl or carboxyl groups (Benedik et al., 1998; Bressler and Gray, 2002; Riddle et al., 2003). Previously suggested degradation pathways

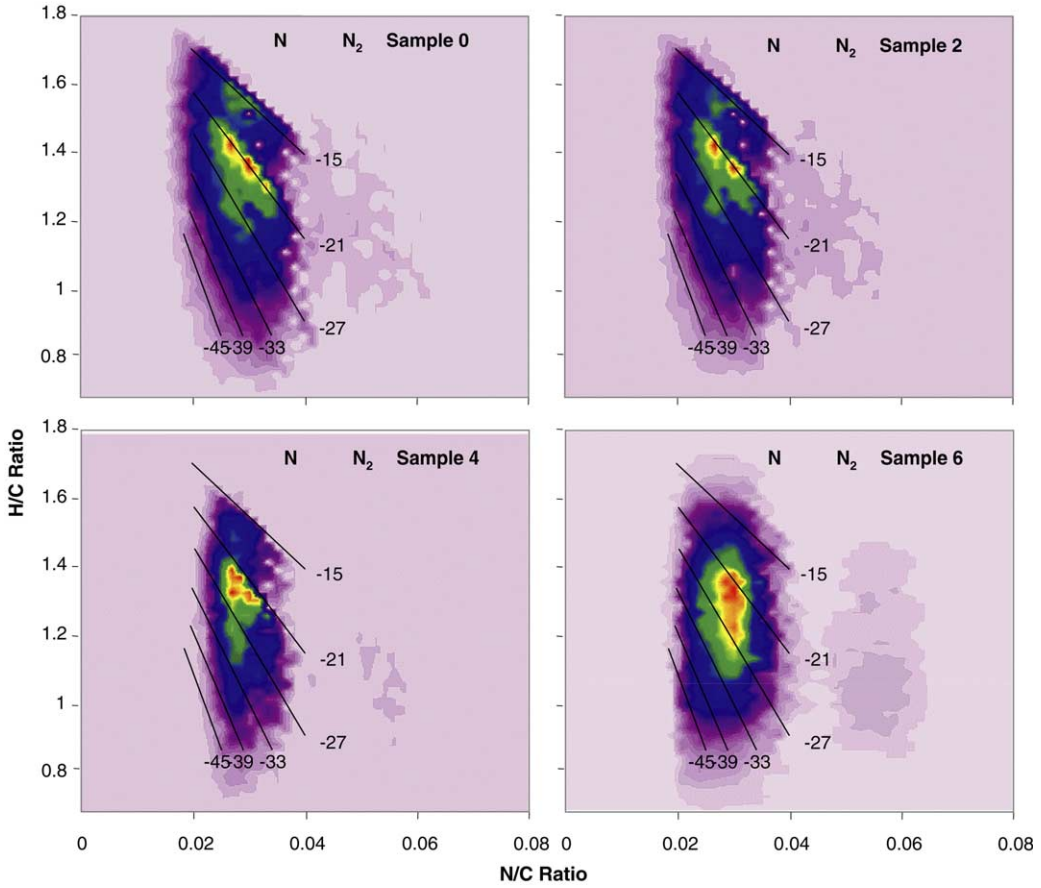

Fig. 10. 3D van Krevelen diagram of nitrogen-containing compounds identified in non-degraded (sample 0), slight-moderately degraded (sample 2), severely degraded (sample 4) and very severely degraded (sample 6) genetically related oils. Normalized ion abundance is color coded by peak height (light purple = minimum, red = maximum). Z-series trend lines for $C_nH_{2n+z}N$ correspond to carbazoles ($Z = -15$, DBE = 12), benzocarbazoles ($Z = -21$, DBE = 15), and higher aromatic carbazoles. Alkylation within individual Z-series increases from right to left.

include NO compounds as intermediates. If that is true, then changes in the NO distributions should be apparent.

The Z-distribution of NO compounds at different stages of degradation is presented in Fig. 12. In the non-degraded sample, NO compounds have a higher DBE distribution than N compounds (Fig. 10, top). The maximum relative abundance exists at a DBE value of 18 ($Z = -33$) for non-degraded oil sample. As the biodegradation proceeds, the distributions of DBE values for NO compounds shift to lower numbers. Although the abundance of NO compounds decreases substantially for more degraded samples (Fig. 4), the relative magnitude of NO compounds with lower DBE values ($Z = -19$ to -23) actually increases (Fig. 12). This trend strongly suggests that the degradation pathway of nitrogen-containing aromatic compounds includes a ring-opening reaction that decreases DBE.

4.4. Sulfur containing compounds

The oils contain a diverse group of sulfur classes, ranging from S_1O_1 to S_1O_9 (not shown). The S_1O_3 species, which may be SO species with an O_2 acid group, are the most abundant in the non-degraded oil. These compounds decline rapidly in relative abundance with increasing biodegradation and are not detected in the severely biodegraded oils. S_1O_2 species behave like S_1O_3 species, but are not completely removed in the severely degraded oils. In contrast, the S_1O_1 species, which are nearly absent in the non-degraded oil, increase in relative abundance with biodegradation (Fig. 4).

It is unlikely that the destruction of the S_1O_2 and higher oxygenated species is related to the generation (or preservation) of the S_1O species. The increased abundance of the S_1O_1 species may originate from the oxidation of S_1 sulfides or from the sulfurization of O_1

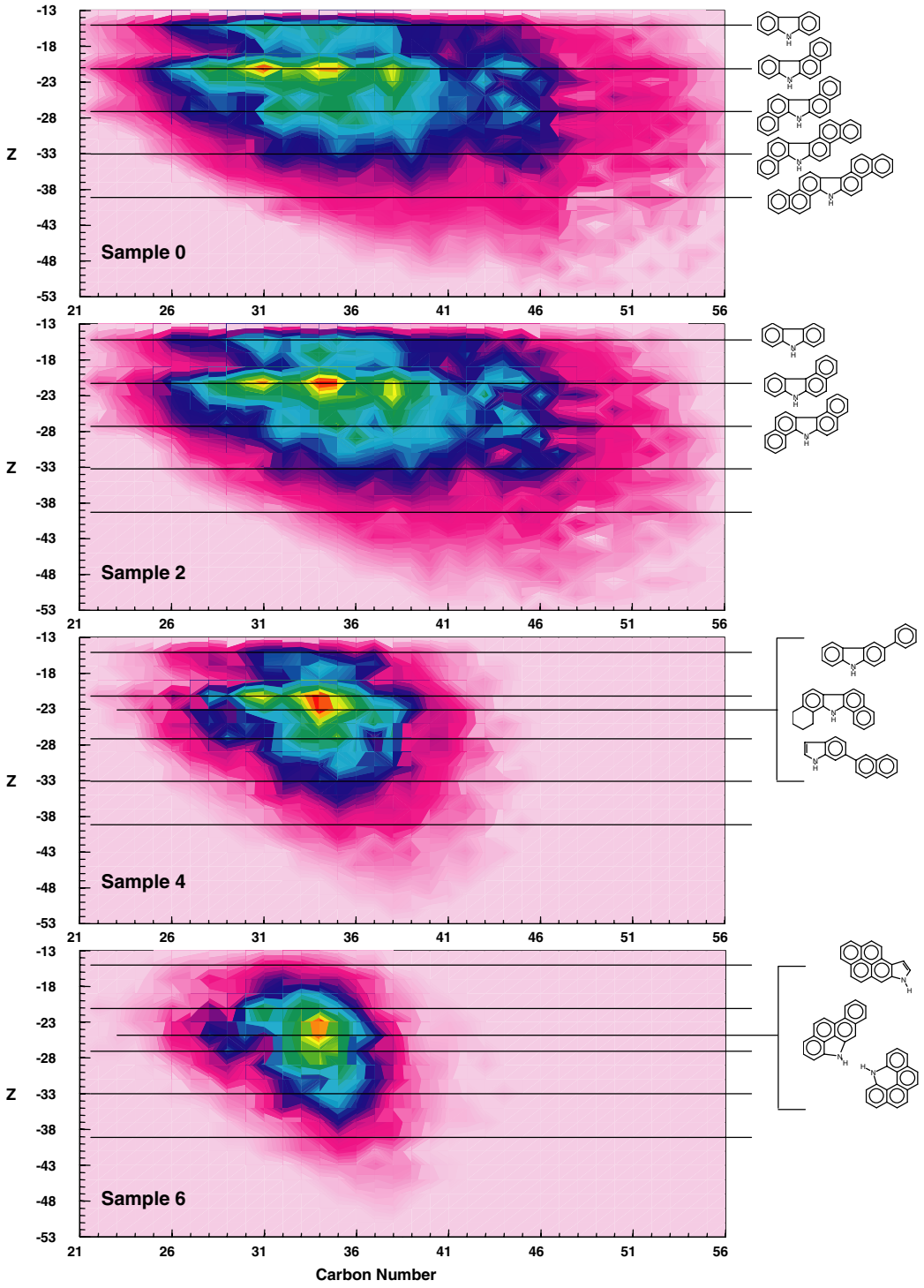

Fig. 11. Relative abundances of N_1-species as a function of Z-number and carbon number in non-degraded (sample 0), slight-moderately degraded (sample 2), severely degraded (sample 4) and very severely degraded (sample 6) genetically related oils. Normalized ion abundance is color coded by peak height (light purple = minimum, red = maximum). Representative Z-series trend lines for $C_nH_{2n+z}N$ correspond to carbazoles ($Z = -15$, DBE = 12), benzocarbazoles ($Z = -21$, DBE = 15), and higher benzocarbazoles ($Z = -27$ and -33, DBE = 18 and 21, respectively). The severely biodegraded oils appear to be enriched in shielded and more condensed pyrrolic structures.

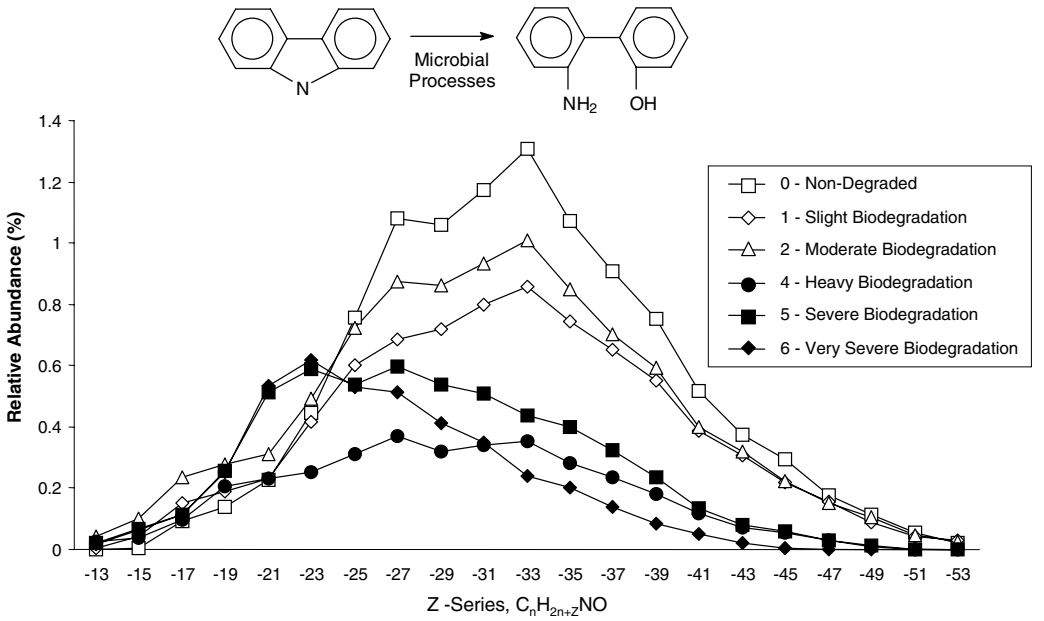

Fig. 12. Relative abundance for various Z-series for $C_nH_{2n+z}NO$ compounds (^{12}C and ^{13}C isomers are combined). Although the overall abundance of NO-species decreases within increasing biodegradation, the abundance of low DBE NO compounds increases, suggesting that microbial processes form these species as intermediate metabolites.

compounds. The latter could occur if sulfate-reducing bacteria are involved in the degradation process.

5. Conclusions

A common perception is that the biodegradation of crude oils occurs in a quasi-stepwise fashion and that the NSO compounds are relatively bioresistant. This conclusion is based on observations of saturated and aromatic hydrocarbons, which are mineralized at different rates as biodegradation proceeds, and on the apparent enrichment of the polar and asphaltene fractions as the hydrocarbons are removed. The increased abundance of naphthenic acids tends to offset any degradation of NSO compounds.

By examining the entire suite of acidic and neutral nitrogen polar compounds by ultrahigh-resolution mass spectrometry, we demonstrate that these polar compounds are not as bioresistant as once believed and that these compounds undergo selective degradation processes as complex as those for hydrocarbons.

Microbial alteration is observed to occur in all compound classes with preferential removal of specific species. Compounds with a high degree of alkylation, presumably associated with long alkyl side chains, are removed from all compound series under conditions associated with moderate (saturated biomarkers unaffected) to severe biodegradation. Some compound series, such as O_1, O_3, and SO_{3-9}, are mineralized under conditions of mild biodegradation (*n*-alkanes, isoprenoids still present). Changes in the Z-series and alkyl distributions of the O_2 species result from simultaneous microbial degradation and generation. Acyclic fatty acids are the predominant O_2 species in the non-degraded oil. These compounds are mineralized under mild conditions, during which the $Z = -10$ series, likely to be hopanoic acids, become the most abundant. Changes in the alkyl distributions of the $Z = -10$ O_2 species agree well with prior observations on hopanoic acids in biodegraded oil and reflect the generation of demethylated species in the most degraded sample. The potential of using ESI–FTICR to monitor polar biomarkers in petroleum without sample derivatization and fractionation is demonstrated. Naphthenic acids with 2-, 3- and 4-rings increasingly dominate the O_2-species, as biodegradation becomes severe and saturated naphthenic structures are mineralized. The acyclic/cyclic (A/C) ratio [$\Sigma O_{2\ Z=0}/\Sigma O_{2\ Z=-4,\ -6,\ -8}$] offers a new way to quantitate the degree of biodegradation.

Acknowledgements

We thank Daniel McIntosh for machining all of the custom parts required for the 9.4 T instrument construction, Mark R. Emmett and John P. Quinn for design and construction of the microelectrospray source, and Christopher L. Hendrickson for help in optimizing instrument operating parameters. We also thank John

Okafor, Phuc Nguyen and Frank Chen of ExxonMobil Upstream Research Company for conducting the supporting geochemical analysis. This work was supported by the NSF National High Field FT–ICR Facility (CHE-99-09502), Florida State University, the National High Magnetic Field Laboratory in Tallahassee, FL and ExxonMobil Research and Engineering Company. Finally, we thank Barry Bennett and a second anonymous reviewer for their careful proofing and helpful suggestions.

Associate Editor—**Martin Fowler**

References

Behar, F.H., Albrecht, P., 1984. Correlations between carboxylic acids and hydrocarbons in several crude oils; alteration by biodegradation. Organic Geochemistry 6, 597–604.

Benedik, M.J., Gibbs, P.R., Riddle, R.R., Willson, R.C., 1998. Microbial denitrogenation of fossil fuels. Trends in Biotechnology 16, 390–395.

Blakney, G.T., vanderRest, G., Johnson, J.R., Freitas, M.A., Drader, J.J., Shi, S.D.-H., Hendrickson, C.L., Kelleher, N.L., Marshall, A.G., 2001. Further improvements to the MIDAS data station for FT–ICR mass spectrometry. In: 49th ASMS Conference on Mass Spectrometry and Allied Topics, p. WPM265, Chicago, IL.

Bressler, D.C., Gray, M.R., 2002. Hydrotreating chemistry of model products from bioprocessing of carbazoles. Energy and Fuels 16, 1076–1086.

Budzinski, H., Raymond, N., Nadalig, T., Gilewicz, M., Garrigues, P., Bertrand, J.C., Caumette, P., 1998. Aerobic biodegradation of alkylated aromatic hydrocarbons by a bacterial community. Organic Geochemistry 28, 337–348.

Connan, J., 1984. Biodegradation of crude oils in reservoirs. In: Brooks, J., Welte, D.H. (Eds.), Advances in Petroleum Geochemistry 1. Academic Press, London, pp. 299–335.

Emmett, M.R., White, F.M., Hendrickson, C.L., Shi, S.D.-H., Marshall, A.G., 1998. Application of micro-electrospray liquid chromatography techniques to FT–ICR MS to enable high-sensitivity biological analysis. Journal of the American Society for Mass Spectrometry 9, 333–340.

Head, I.M., Jones, D.M., Larter, S.R., 2003. Biological activity in the deep subsurface and the origin of heavy oil. Nature 426, 344–352.

Hendrickson, C.L., Quinn, J.P., Emmett, M.R., Marshall, A.G., 2000. Quadrupole mass filtered external accumulation for Fourier transform ion cyclotron resonance mass spectrometry. In: 48th ASMS Conference on Mass Spectrometry and Allied Topics, p. MP083, Long Beach, CA.

Holba, A.G., Huizinga, B.J., Wright, L., Scheihing, M.H., Dzou, L.I., Hickey, J.J., Franks, S.G., 2004. Effects and impact of early and late stage anaerobic biodegradation. In: AAPG-SEPM National Meeting, p. A65, Dallas, TX..

Huang, H., Bowler, B.F.J., Zhang, Z., Oldenburg, T.B.P., Larter, S.R., 2003. Influence of biodegradation on carbazole and benzocarbazole distributions in oil columns from the Liaohe basin, NE China. Organic Geochemistry 34, 951–969.

Hughey, C.A., Hendrickson, C.L., Rodgers, R.P., Marshall, A.G., 2001a. Elemental composition analysis of processed and unprocessed diesel fuel by electrospray ionization Fourier transform ion cyclotron resonance mass spectrometry. Energy and Fuels 15, 1186–1193.

Hughey, C.A., Hendrickson, C.L., Rodgers, R.P., Marshall, A.G., Qian, K.N., 2001b. Kendrick mass defect spectrum: a compact visual analysis for ultrahigh-resolution broadband mass spectra. Analytical Chemistry 73, 4676–4681.

Hughey, C.A., Rodgers, R.P., Marshall, A.G., 2002a. Resolution of 11,000 compositionally distinct components in a single electrospray ionization Fourier transform ion cyclotron resonance mass spectrum of crude oil. Analytical Chemistry 74, 4145–4149.

Hughey, C.A., Rodgers, R.P., Marshall, A.G., Qian, K.N., Robbins, W.K., 2002b. Identification of acidic NSO compounds in crude oils of different geochemical origins by negative ion electrospray Fourier transform ion cyclotron resonance mass spectrometry. Organic Geochemistry 33, 743–759.

Hughey, C.A., Rodgers, R.P., Marshall, A.G., Walters, C.C., Qian, K., Mankiewicz, P., 2004. Acidic and neutral polar NSO compounds in Smackover oils of different thermal maturity revealed by electrospray high field Fourier transform ion cyclotron resonance mass spectrometry. Organic Geochemistry 35, 863–880.

Hunt, J.H., 1995. Petroleum Geology and Geochemistry, second ed. W.H. Freeman and Co..

Isaksen G.H, 1996. Organic geochemistry and geohistory of the Triassic succession of Bjørnøya, Barents Sea. Organic Geochemistry 24, 333–349.

Jaffé, R., Gallardo, M.T., 1993. Application of carboxylic acid biomarkers as indicators of biodegradation and migration of crude oils from the Maracaibo Basin, western Venezuela. Organic Geochemistry 20, 973–984.

Jenisch-Anton, A., Adam, P., Albrecht, P., 2000. Molecular evidence for biodegradation of geomacromolecules. Geochimica et Cosmochimica Acta 64, 3525–3537.

Kendrick, E., 1963. A mass scale based on $CH_2 = 14.0000$ for high resolution mass spectrometry of organic compounds. Analytical Chemistry 35, 2146–2154.

Kim, S., Kramer, R.W., Hatcher, P.G., 2003a. Graphical method for analysis of ultrahigh-resolution broadband mass spectra of natural organic matter, the van Krevelen diagram. Analytical Chemistry 75, 5336–5344.

Kim, S., Simpson, A.J., Kujawinski, E.B., Freitas, M.A., Hatcher, P.G., 2003b. High resolution electrospray ionization mass spectrometry and 2D solution NMR for the analysis of DOM extracted by C_{18} solid phase disk. Organic Geochemistry 34, 1325–1335.

Kujawinski, E.B., Freitas, M.A., Zang, X., Hatcher, P.G., Green-Church, K.B., Jones, R.B., 2002. The application of electrospray ionization mass spectrometry (ESI MS) to the structural characterization of natural organic matter. Organic Geochemistry 33, 171–180.

Larter, S., Wilhelms, A., Head, I., Koopmans, M., Aplin, A., Di Primio, R., Zwach, C., Erdmann, M., Telnaes, N., 2003. The controls on the composition of biodegraded oils in the

deep subsurface-part 1: biodegradation rates in petroleum reservoirs. Organic Geochemistry 34, 601–613.

Ledford Jr., E.B., Rempel, D.L., Gross, M.L., 1984. Space-charge effects in Fourier-transform mass spectrometry. II Mass calibration. Analytical Chemistry 56, 2744–2748.

Mackenzie, A.S., Wolff, G.A., Maxwell, J.R., 1983. Fatty acids in some biodegraded petroleums; possible origins and significance. In: Bjorøy, M., Albrecht, C., Cornford, C., deGroot, K., Eglinton, G., Galimov, E., Leythaeuser, D., Pelet, R., Rullkötter, J., Speers, G. (Eds.), Advances in Organic Geochemistry 1981. Wiley, Chichester-New York, pp. 637–649.

Marshall, A.G., Hendrickson, C.L., Jackson, G.S., 1998. Fourier transform ion cyclotron resonance mass spectrometry: a primer. Mass Spectrometry Reviews 17, 1–35.

Meredith, W., Kelland, S.J., Jones, D.M., 2000. Influence of biodegradation on crude oil acidity and carboxylic acid composition. Organic Geochemistry 31, 1059–1073.

Nascimento, L.R., Rebouças, L.M.C., Koike, L., de A.M Reis, F., Soldan, A.L., Cerqueira, J.R., Marsaioli, A.J., 1999. Acidic biomarkers from Albacora oils, Campos Basin, Brazil. Organic Geochemistry 30, 1175–1191.

Peters, K.E., Moldowan, J.M., McCaffrey, M.A., Fago, F.J., 1996. Selective biodegradation of extended hopanes to 25-norhopanes in petroleum reservoirs. Insights from molecular mechanics. Organic Geochemistry 24, 765–783.

Peters, K.E., Walters, C.C., Moldowan, J.M., 2004. The Biomaker Guide, Second ed. Biomakers and Isotopes in Petroleum Exploration and Earth History, Volume 2 Cambridge University Press.

Pineda-Flores, G., Boll-Argüello, G., 2004. A microbial consortium isolated from a crude oil sample that uses asphaltenes as a carbon and energy source. Biodegradation 15, 145–151.

Prince, R.C., 2002. Petroleum and other hydrocarbons, biodegradation of. In: Britton, G. (Ed.), Encyclopedia of Environmental Microbiology. John Wiley, New York, pp. 2402–2416.

Qian, K., Rodgers, R.P., Hendrickson, C.L., Emmett, M.R., Marshall, A.G., 2001a. Reading chemical fine print: resolution and identification of 3000 nitrogen-containing aromatic compounds from a single electrospray ionization Fourier transform ion cyclotron resonance mass spectrum of heavy petroleum crude oil. Energy and Fuels 15, 492–498.

Qian, K.N., Robbins, W.K., Hughey, C.A., Cooper, H.J., Rodgers, R.P., Marshall, A.G., 2001b. Resolution and identification of elemental compositions for more than 3000 crude acids in heavy petroleum by negative-ion microelectrospray high-field Fourier transform ion cyclotron resonance mass spectrometry. Energy and Fuels 15, 1505–1511.

Riddle, R.R., Gibbs, P.R., Willson, R.C., Benedik, M.J., 2003. Recombinant carbazole-degrading strains for enhanced petroleum processing. Journal of Industrial Microbiology and Biotechnology 30, 6–12.

Rowland, S.J., Alexander, R., Kagi, R.I., Jones, D.M., Douglas, A.G., 1986. Microbial degradation of aromatic components of crude oils; a comparison of laboratory and field observations. Organic Geochemistry 9, 153–161.

Senko, M.W., Canterbury, J.D., Guan, S., Marshall, A.G., 1996a. A high-performance modular data system for Fourier transform ion cyclotron resonance mass spectrometry. Rapid Communications in Mass Spectrometry 10, 1839–1844.

Senko, M.W., Hendrickson, C.L., Paša-Tolic, L., Marto, J.A., White, F.M., Guan, S., Marshall, A.G., 1996b. Electrospray ionization Fourier transform ion cyclotron resonance at 9.4 T. Rapid Communications in Mass Spectrometry 10, 1824–1828.

Senko, M.W., Hendrickson, C.L., Emmett, M.R., Shi, S.D.-H., Marshall, A.G., 1997. External accumulation of ions for enhanced electrospray ionization Fourier transform ion cyclotron resonance mass spectrometry. Journal of the American Society for Mass Spectrometry 8, 970–976.

Shi, S.D.-H., Drader, J.J., Freitas, M.A., Hendrickson, C.L., Marshall, A.G., 2000. Comparison and interconversion of the two most common frequency-to-mass calibration functions for Fourier transform ion cyclotron resonance mass spectrometry. International Journal of Mass Spectrometry 195–196, 591–598.

Sjoblom, J., Aske, N., Auflem, I.H., Brandal, O., Havre, T.E., Saether, O., Westvik, A., Johnsen, E.E., Kallevik, H., 2003. Our current understanding of water-in-crude oil emulsions. Recent characterization techniques and high pressure performance. Advances in Colloid and Interface Science 100, 399–473.

Slavcheva, E., Shone, B., Turnbull, A., 1999. Review of naphthenic acid corrosion in oil refining. British Corrosion Journal 34, 125–131.

Stenson, A.C., Landing, W.M., Marshall, A.G., Cooper, W.T., 2002. Ionization and fragmentation of humic substances in electrospray ionization Fourier transform ion cyclotron resonance mass spectrometry. Analytical Chemistry 74, 4397–4409.

Sundararaman, P., Hwang, R.J., 1993. Effect of biodegradation on vanadylporphyrin distribution. Geochimica et Cosmochimica Acta 57, 2283–2290.

Thorn, K.A., Aiken, G.R., 1998. Biodegradation of crude oil into nonvolatile organic acids in a contaminated aquifer near Bemidji, Minnesota. Organic Geochemistry 29, 909–931.

Tomczyk, N.A., Winans, R.E., Shinn, J.H., Robinson, R.C., 2001. On the nature and origin of acidic species in petroleum. 1. Detailed acid type distribution in a California crude oil. Energy and Fuels 15, 1498–1504.

Townsend, G.T., Prince, R.C., Suflita, J.M., 2004. Anaerobic biodegradation of alicyclic constituents of gasoline and natural gas condensate by bacteria from an anoxic aquifer. FEMS Microbiology Ecology 49, 129–135.

Volkman, J.K., Alexander, R., Kagi, R.I., Woodhouse, G.W., 1983. Demethylated hopanes in crude oils and their applications in petroleum geochemistry. Geochimica et Cosmochimica Acta 47, 785–794.

Watson, J.S., Jones, D.M., Swannell, R.P.J., van Duin, A.C.T., 2002. Formation of carboxylic acids during aerobic biodegradation of crude oil and evidence of microbial oxidation of hopanes. Organic Geochemistry 33, 1153–1169.

Wenger, L.M., Davis, C.L., Isaksen, G.H., 2002. Multiple controls on petroleum biodegradation and impact on oil quality. SPE Reservoir Evaluation and Engineering 5, 375–383.

Widdel, F., Rabus, R., 2001. Anaerobic biodegradation of saturated and aromatic hydrocarbons. Current Opinion in Biotechnology 12, 259–276.

Wu, Z.G., Jernstrom, S., Hughey, C.A., Rodgers, R.P., Marshall, A.G., 2003. Resolution of 10,000 compositionally distinct components in polar coal extracts by negative-ion electrospray ionization Fourier transform ion cyclotron resonance mass spectrometry. Energy and Fuels 17, 946–953.

Zhan, D., Fenn, J.B., 2000. Electrospray mass spectrometry of fossil fuels. International Journal of Mass Spectrometry 194, 197–208.